Biophysical Journal Volume 105 December 2013 2507–2516

Conformational Dynamics of Calcium-Triggered Activation of Fusion by Synaptotagmin

Shyam S. Krishnakumar,* Daniel Kümmel, Sunny J. Jones, Daniel T. Radoff, Karin M. Reinisch, and James E. Rothman*

Department of Cell Biology, Yale University School of Medicine, New Haven, Connecticut

ABSTRACT Synaptotagmin triggers rapid exocytosis of neurotransmitters from synaptic vesicles in response to Calcium (Ca^{2+}) ions. Here, we use a novel Nanodisc-based system, designed to be a soluble mimetic of the clamped synaptic vesicle-bilayer junction, combined with fluorescence resonance energy transfer (FRET) spectroscopy to monitor the structural relationships among SNAREs (soluble *N*-ethylmaleimide-sensitive factor attachment protein receptor), Synaptotagmin C2 domains, and the lipid bilayer in real time during the Ca^{2+}-activation process. We report that Synaptotagmin remains rigidly fixed on the partially assembled SNARE complex with no detectable internal rearrangement of its C2 domains, even as it rapidly inserts into the bilayer. We hypothesize that this straightforward, one-step physical mechanism could explain how this Ca^{2+}-sensor rapidly activates neurotransmitter release from the clamped state.

INTRODUCTION

Controlled release of neurotransmitters is central to information processing in the nervous system. To achieve this, synaptic vesicles containing neurotransmitter are already docked at the active zones of the presynaptic membrane (1–3), ready to be triggered to fuse and release their contents into the synapse as Ca^{2+} ions enter the cytoplasm following an action potential (4–6). The release of the neurotransmitter is mediated by soluble *N*-ethylmaleimide-sensitive factor attachment protein receptor (SNARE) proteins, which directly catalyze the fusion of the synaptic vesicles to the plasma membrane (7–9). Complexin (CPX) synchronizes neurotransmitter release by arresting the SNARE assembly process, when the v-SNAREs (VAMP2) are almost half assembled (10,11). X-ray crystal structure of this intermediate state (12) shows that CPX does this by bridging from one SNARE complex to another. It inserts its accessory helix (CPX_{acc}) into the adjacent t-SNAREs (Syntaxin/SNAP25) to sterically prevent further zippering of its v-SNARE, and this *trans*-interaction could generate a zig-zag array of half-zippered SNARE complexes at the docked vesicle-bilayer interface (12).

Synaptic vesicle protein Synaptotagmin 1 (SYT1) is the principal Ca^{2+} sensor that triggers release of neurotransmitters (13–18). SYT1 acts on *trans*-SNARE complexes (SNAREpins) that are held in a half-zippered state by CPX (10–12,19), to release this clamp and allow the SNAREs to rapidly complete their zippering and release the neurotransmitter (10,20). How Ca^{2+} binding to Synaptotagmin couples to the SNARE complex to achieve this, the very crux of the release process, is still a mystery (21). It is well established that when SYT1 binds Ca^{2+} ions, the adjacent surface loops on each of the C2 domains (C2A and C2B) are partially inserted into the membrane bilayer containing acidic lipids such as phosphatidylserine (PS) and phosphatidylinositol 4,5-bisphosphate (PIP_2) (22–28), an event that activates fusion (29,30) and is physiologically required for triggering synaptic transmission (13,31–33). Although this process, really the power stroke of SYT1, is clearly a vital step needed for the release (31–33), and may well accelerate fusion (30,34), it is in itself insufficient for fusion because without SNAREs, SYT1 does not fuse membranes.

How, then, does this Ca^{2+}-triggered power stroke trigger SNAREs to complete their assembly and initiate fusion? There are two alternative possibilities—either the two C2 domains (each of which separately binds Ca^{2+} and inserts into membranes) rearrange on the surface of the SNARE complex, triggering a linked rearrangement of the SNAREs that enables the zippering to continue, or there is no conformational rearrangement in SYT1 upon binding Ca^{2+}, but rather SYT1 acts as a rigid molecule and exerts force by pulling on the attached SNAREs as its loops insert into the vesicle or the plasma membrane, perturbing the clamped SNAREpins, and triggering its full assembly.

Here, we address this question using, what we believe to be a novel system that allowed us to investigate the dynamics of SYT1 on SNAREpins during the Ca^{2+}-activation process—Nanodiscs of membrane that are joined by partly assembled SNAREpins. This readily manipulated, soluble mimetic of synaptic vesicle-target membrane junctions enabled us to obtain precise real-time structural measurements of substeps in the process of Ca^{2+} activation on a millisecond timescale and propose a simple physical model of how this process occurs.

Submitted May 11, 2013, and accepted for publication October 23, 2013.

*Correspondence: shyam.krishnakumar@yale.edu or james.rothman@yale.edu

Editor: Axel Brunger.

0006-3495/13/12/2507/10 $2.00

http://dx.doi.org/10.1016/j.bpj.2013.10.029

MATERIALS AND METHODS

Plasmid constructs and protein purification

The constructs used in this study are t-SNARE complex containing full-length mouse SNAP25 (residues 1–206) and rat ΔN Syntaxin-1 mutant (kindly provided by Dr. Jingshi Shen, University of Colorado) that lacks the N-terminal domain (residues 151–288) (35), full-length mouse VAMP2-wild-type (WT) (VAMP2 residues 1–116) or VAMP2-4X (VAMP2 residues 1–116 with mutations L70D, A74R, A81D, and L84D) (12,36), Complexin (human Complexin1 residues 1–134) (36), soluble Synaptotagmin (rat Synaptotagmin-1 residues 92–421) (37), and MSP1E3D1 expression vector (pMSP1E3D1) purchased from Addgene (Cambridge, MA) (38). All constructs were expressed and purified as described previously (12,36–38). With exception of the t-SNAREs and CPX, which were eluted from Ni-NTA beads with Imidazole, the other proteins were cleaved off the beads to remove the His-tag (SUMO protease for VAMPs; TEV protease for MSPE3D1) or the GST-tag (Thrombin for SYT1). If needed, the proteins were further purified by ion exchange (Mono-Q or Mono-S affinity column) or by size exclusion chromatography (Hi-Load Superdex 75, GE Healthcare, Piscataway, NJ).

Labeling with fluorescent dyes

For site-specific labeling with fluorophores, cysteines were introduced into t-SNAREs (SNAP25 residues 20, 55, 76, 80, and 193), VAMP2-4X (residue 28, 54, 56, and 86), CPX (residue 38), Synaptotagmin (positions 154, 234, 254/396, 304, and 383) using the Quickchange (Stratagene, Santa Clara, CA) Mutagenesis kit. Thiol-reactive fluorescent probes Oregon Green (OG) 488 Maleimide, Texas Red (TR) C5 Bromoacetamide, IANBD amide (*N*,*N*′-Dimethyl-*n*-(Iodoacetyl)-*N*′-(7-nitrobenz-2-oxa-1,3-diazol-4-yl) Ethylenediamine), Stilbene (4-acetamido-4′-((iodoacetyl)amino)-stilbene-2,2′-disulfonic acid, disodium salt), and Bimane (Monochlorobimane) were purchased from Life Technologies (Grand Island, NY). The proteins were mixed with 10X molar excess of the appropriate dye in 25 mM HEPES, pH 7.4, 140 mM KCl, 10% Glycerol, 1 mM TCEP (containing 1% octylglucoside for full-length VAMP2-4X (or WT) and t-SNAREs). Following the overnight incubation at 4°C, the excess dye was separated from the labeled proteins using a NAP desalting column (GE Healthcare). Typically, a single pass through the NAP5 column was sufficient for efficient removal of free dye, but in a few cases (<5%) the sample was passed over the NAP5 column a second time. The ratio of the concentration of the dye (calculated from the absorbance value at its excitation maxima from its extinction coefficient) and that of the protein (from Bradford assay) was used to calculate the labeling efficiency. In all cases, the labeling efficiency was >80%. All steady-state fluorescence data were obtained on a Perkin-Elmer (Waltham, MA) LS55 luminescence spectrometer operating at 25°C. The rapid mixing stopped flow analysis was done using Applied Photophysics (Surrey, United Kingdom) SX.18 MV stopped-flow spectrometer at 25°C.

Nanodisc preparation

Nanodiscs containing v-SNAREs (v-disc) or t-SNAREs (t-disc) were prepared as described earlier (38). Briefly, lipid mixture of palmitoyl-2-oleoyl phosphatidylcholine (POPC): 1,2 dioleoyl phosphatidylserine (DOPS) at 85:15 (for standard preparation, changed under specific conditions) was dried under nitrogen flow, followed by vacuum for 1 h. The lipid film was suspended in reconstitution buffer (25 mM HEPES, pH 7.4, 140 mM KCl) with membrane scaffold protein (MSP) and VAMPs or t-SNAREs containing 1% octylglucoside by rapid mixing at room temperature for 15–30 min. The protein lipid ratios were MSP:SNAREs:Lipid = 2:8:120 (for v-discs) and 2:1:120 (for t-discs). The samples were incubated at 4°C for 3 h with mild shaking, and SM-2 bio-beads were then added and incubated overnight to remove the excess detergent. The assembled nanodiscs containing the SNARE proteins were separated from unincorporated proteins and empty nanodiscs by gel filtration (Superdex 200 column, Fig. S1 in the Supporting Material). The samples were concentrated and analyzed by SDS PAGE-Coomassie stain (Fig. S1). The number of VAMP2-4X and t-SNAREs per disc was determined by the VAMP/MSP ratio according to the quantification of the protein bands. On an average, the v-discs contain 8.1 ± 0.8 copies of VAMP2-4X per disc and t-disc has 0.88 ± 0.3 copies of t-SNARE per disc. (Note: For quantification purposes, the t-discs were further purified using Ni^{2+}-NTA beads and imidazole elution.) All lipids were purchased from Avanti Polar Lipids (Alabaster, AL).

FRET assay to monitor SNARE assembly

To follow the assembly of SNARE complex between the Nanodiscs, 1 μM of OG 488 (donor) labeled t-discs and TR (acceptor) labeled VAMP2 or VAMP2-4X containing Nanodiscs were mixed in 25 mM HEPES pH 7.4, 140 mM KCl, 10% Glycerol, 1 mM TCEP buffer, and the FRET signal at 615 nm (when excited at 475 nm) was measured for 1 h at 37°C. As a control, 10 μM of the cytoplasmic domain of VAMP2 (CDV) was included to titrate out t-SNAREs and block assembly. FRET between fluorophores attached at the N-terminus (SNAP25 D20C/VAMP R28C), middle (SNAP25 E55C/VAMP R56C), and C-terminus (SNAP25 D80C/VAMP R86C) were measured. The labeling efficiency (N-terminus to C-terminus) was 96%, 93%, and 95% for OG 488 and 83%, 86%, and 82% for TR. To verify that the FRET signal is not affected by the labeling position, the FRET assay was carried out using free SNARE proteins in 25 mM HEPES buffer containing 1% octylglucoside.

Assembly of prefusion SNARE complex

To assemble the prefusion SNARE complex, t-discs were mixed with v-discs at 1:3 molar ratio (Complexin was included for CPX-SNARE4X complex at the same concentration of v-discs). Following an overnight incubation at 4°C, the assembled complexes were purified on Ni-NTA beads using the oligohistidine tag on t-SNAREs (only t-SNAREs have the His_6 tag because VAMPs and MSP were purified by protease cleavage). The beads were washed with 20X column volume of buffer (25 mM HEPES, pH 7.4 140 mM KCl, 10% Glycerol, 1 mM TCEP), and the complexes were eluted off the beads using the same buffer containing 400 mM imidazole. The formation of the SNARE4X (or CPX-SNARE4X) complex was verified by Western blot analysis using antibody against VAMP2 (and CPX) (Fig. S1). The samples were then dialyzed against 25 mM HEPES, pH 7.4, 50 mM KCl, 10% Glycerol, 1 mM TCEP buffer to remove the excess imidazole.

Complexin binding analysis

CPX binding and its conformational state were followed using the Stilbene-Bimane FRET pair as described earlier (12,36). CPX-SNARE4X complexes (or CPX-SNARE complex) were assembled with CPX labeled at residue 38 in the accessory helix with Bimane and t-discs labeled with Stilbene on SNAP25 residue 193. The quenching of donor fluorescence at 410 nm was used to follow the conformational state of the CPX accessory helix.

Synaptotagmin binding analysis

To test the binding of SYT1 to prefusion CPX-SNARE complex under Ca^{2+}-free conditions, 2.5 μM of SYT1 labeled with TR on either C2A (residue 154) or C2B (residue 383) was mixed with 0.1 μM of preassembled CPX-SNARE4X on Nanodisc (100% PC lipids) labeled with OG 488 on SNAP25 residue 76 in 25 mM HEPES, pH 7.4, 50 mM KCl, 10% Glycerol, 1 mM TCEP containing 0.2 mM EGTA. Following a 3 h incubation at 37°C,

fluorescence emission spectra were collected between 495 and 650 nm with the excitation wavelength set at 475 nm. A sample containing unlabeled SYT1 was used to obtain the donor-only signal. The emission spectra were corrected for contributions from buffers and acceptor-only samples.

Calculation of synaptotagmin binding affinities

To measure the affinities of the SYT1 to t-discs or different SNARE complexes (± CPX) on Nanodiscs under Ca^{2+}-free conditions, varying concentrations of SYT1 (0.1–8 μM) labeled with TR on its C2B domain (position 383) was mixed with 0.1 μM of t-disc or preassembled SNARE complexes (±CPX) labeled with OG 488 on SNAP25 residue 76 and incubated for minimum 3 h at 37°C in 25 mM HEPES, pH 7.4, 50 mM KCl, 10% Glycerol, 1 mM TCEP containing 0.2 mM EGTA. For affinity measurements in the presence of Calcium, 1.2 mM Ca^{2+} (1 mM free Ca^{2+}) was included before the incubation step. Following the incubation, the fluorescence emission spectra (495–660 nm) were collected with excitation set at 475 nm. The donor fluorescence at 515 nm was corrected for both the direct excitation of acceptor itself and for inner filter effect (39) in addition to buffer correction. The apparent binding affinity (K_d) was calculated assuming a single (1:1) binding model using the equation:

$$\frac{Fo-F}{Fo-Fc}=\frac{[\mathrm{P}]+[\mathrm{L}]+K_\mathrm{d}-\sqrt{([P]+[L]+K_d)^2-4*[P]*[L]}}{2*[P]},$$

where F is measured fluorescence, Fo is the starting fluorescence, Fc is the fluorescence of fully assembled complex (i.e., the maximal quenching observed with 20 μM SYT1), $[P]$ is the concentration of SNARE complexes used, and $[L]$ is the added concentration of SYT1 (40).

Ca^{2+}-triggered membrane interaction of synaptotagmin

To monitor Synaptotagmin-membrane interaction, the tips of the Ca^{2+} binding loops of both C2 domains (residue 234 on C2A and residue 304 on C2B) were labeled with an environment-sensitive probe, NBD (7-nitrobenz-2-oxa-1,3-diazol-4-yl)ethylenediamine). SYT1-CPX-SNARE4X complex (0.25 μM of NBD-labeled SYT1 incubated with 2.5 μM of preformed CPX-SNARE4X complex on Nanodiscs containing 15% DOPS for 3 h at 37°C or overnight at 4°C) was assembled in 25 mM HEPES, pH 7.4, 50 mM KCl, 10% Glycerol, 1 mM TCEP containing 0.2 mM EGTA. For steady-state measurements, the samples were mixed with equal volume of either buffer containing EGTA or Ca^{2+} (yielding a final concentration of 0.2 mM EGTA or 1mM of free Ca^{2+}) and the fluorescence emission spectra (485–650 nm, Ex 460 nm) were recorded. To follow the dynamics of this process, we used the rapid mixing stopped-flow technique with preassembled NBD-labeled SYT1-CPX-SNARE4X loaded into one syringe and buffer containing EGTA or Ca^{2+} in the other syringe. The samples were mixed rapidly (dead time ~1 msec) yielding a final concentration of 0.2 mM EGTA and 1 mM Ca^{2+}. The change in fluorescence signal collected with a 510 nm cutoff filter (Ex 460 nm) was fitted with a single exponential function to calculate the observed rate of insertion of the Ca^{2+}-loops.

Preferential membrane interaction studies

To determine which lipid bilayer SYT1 inserts into, we assembled v-and t-discs with lipid compositions that accurately reflects the synaptic vesicle and plasma membrane, respectively. The lipid compositions were 32% POPC, 15% DOPS, 25% POPE, 25% Cholesterol, and 3% PI for v-discs and 35% POPC, 15% DOPS, 21.5% POPE, 25% Cholesterol, 3% PI with a varying amount of PIP2 (1.5%, 3%,and 6%) for the t-discs. SYT1-CPX-SNARE4X Nanodiscs were assembled as described previously and the % quenching of NBD signal by Rhodamine-PE (1.5%) introduced into either the v- or the t-discs was used to follow the preferential interaction. The percent quenching of the NBD fluorescence under each lipid composition was normalized to the maximum quenching observed for the same lipid composition under noncompeting conditions to calculate the percentage of the Synaptotagmin inserted into each membrane using the formula: $(Q_{sample}-Q_{min})/(Q_{max}-Q_{min})$; where Q_{max}, Q_{min}, and Q_{sample} refers to the maximum quenching observed, minimum quenching observed, and the quenching observed in the sample (see the Supporting Material for additional details).

Effect of calcium addition on SYT1-SNARE interaction

To follow the effect of Ca^{2+} on the SYT1-SNARE interaction, OG 488/TR-labeled SYT1-CPX-SNARE4X complex were assembled as described earlier. The samples were mixed with an equal volume of buffer containing EGTA or Ca^{2+} yielding a final concentration of 0.2 mM EGTA and 1 mM of free Ca^{2+}, and the fluorescence was measured under either steady state (495–650 nm emission spectra, Ex 475 nm) or rapid mixing stopped-flow (510 nm cutoff filter, Ex 475 nm) conditions. To monitor the relative orientation of the C2 domains during the Ca^{2+} activation, the experiments were repeated with SYT1-CPX-SNARE4X complex assembled with SYT1 double-labeled with Alexa 555 and Alexa 647 on position 254 on C2A and 396 on C2B. Fluorescence signal from both the donor channel (550 nm cutoff filter) and acceptor channel (620 nm cutoff filter) excited at 530 nm was collected.

Surface plasmon resonance (SPR) analysis

Binding of SYT1 to isolated CPX containing prefusion (CPX-SNARE60) and postfusion SNARE complexes (CPX-SNARE) was carried out by SPR (Biacore T100, Keck Facility, Yale University). The SNARE complexes (biotinylated by maleimide coupling to Syntaxin 253-Cys) were immobilized on a Streptavidin (SA) chip and SYT1 of increasing concentration was injected over the surface with a high salt (1 M NaCl) regeneration step during each cycle. Amount was SYT1 bound under steady state and a condition was used to calculate the affinity of the SYT1 to the SNARE complexes. The analysis was done under both low salt (50 mM KCl) and normal salt (140 mM KCl) conditions.

RESULTS

Assembly of prefusion *trans*-SNARE complexes between nanodiscs

Nanodiscs consist of a circular fragment of lipids (up to ~17 nm in diameter) encapsulated by two copies of MSP derived from apolipoprotein A1 (38,41). The Nanodiscs contain either multiple copies of the synaptic vesicle v-SNARE, VAMP2 (v-discs) or a single copy of the presynaptic plasma membrane t-SNARE, Syntaxin-SNAP25 (t-discs). When mixed together, the SNAREs bind and assemble between the Nanodiscs, but they do not zipper all the way to fuse the discs due to the topological constraints imposed by the Nanodiscs (Fig. S2). To accurately mimic the prefusion, clamped state of the SNAREpins (11,12) between Nanodiscs (because SNAREs are zippered beyond the prefusion state with WT VAMP2), we employed a previously characterized VAMP2 construct (12,36), which

carries mutations in the C-terminal hydrophobic layers (L70D, A74R, A81D, and L84D; termed VAMP2-4X) that prevent assembly of this region with the t-SNAREs (12,36). FRET between OG 488-labeled SNAP25 on t-discs and TR on VAMP2-4X on v-discs introduced at different position along the SNARE domain (Fig. 1 *A*) showed that the SNAREs indeed are only partially assembled as the extent of the FRET signal was weaker for fluorophores introduced in the C-terminus (SNAP25 D80C/VAMP R86C) compared to the fluorophores attached at the N-terminus (SNAP25 D20C/VAMP R28C) or at the middle (SNAP25 E55C/VAMP R56C) of the SNARE domain (Fig. 1 *A*). Control FRET experiments with full-length VAMP2 in detergent (1% octylglucoside) showed that the maximum FRET achievable with fully formed complexes is similar for all labeling sites (Fig. S2).

Complexin binds to the prefusion *trans*-SNARE complexes (SNARE4X) assembled between Nanodiscs (Fig. S1) and FRET experiments with a Stilbene-Bimane donor-acceptor pair (attached to SNAP25 residue 193 and CPX residue 38 respectively) (12,36) showed that the CPX accessory helix (CPX_{acc}) adopts the open conformation (Fig. 1 *B*, *green curve*). The open conformation is the critical feature of CPX that enables clamping because in this arrangement the accessory helix points away from the assembling four helix SNARE bundle (hence the low FRET signal) where it is positioned to bind to the membrane proximal half of the t-SNARE of an adjacent SNAREpin thereby preventing terminal zippering of its own v-SNARE (12). In fact, the FRET efficiency observed for CPX bound to SNARE4X on Nanodiscs is in excellent agreement with the FRET efficiency observed in the isolated CPX-containing half-zippered SNARE complex (CPX-SNARE60) that was used to determine the x-ray structure (12) of the clamped state (Fig. S3). We conclude that CPX-SNARE4X assembled between the Nanodiscs (Fig. 1 *C*) provides an accurate representation of the state of these proteins in the docked vesicles as predicted by the x-ray structure (12). For comparison, we looked at the binding of CPX to the t-discs alone or *trans*-SNARE complex (assembled with WT VAMP2 on v-discs). In line with our previous findings, we observed no FRET (Fig. 1 *B*, *orange curve*) when CPX was incubated with t-discs alone, and a high FRET signal (Fig. 1 *B*, *red curve*) corresponding to the closed (postfusion) conformation (in which CPX_{acc} runs parallel to the SNARE complex) with *trans*-SNARE complex (12,36).

SYT1 binds to prefusion CPX-SNARE complexes on nanodiscs

SYT1 binds to this mimetic of the (prefusion) clamped SNARE complex in the absence of Ca^{2+} (0.2 mM EGTA), as shown by efficient quenching of the donor fluorescence (OG 488 on SNAP25, residue 76) by acceptor dye (TR) attached to either of the C2 domains (Fig. 2, *A* and *B*). Higher FRET efficiency for the acceptor label on C2B (residue 383, *purple curve*) compared to the C2A (residue 154, *red curve*) label (Fig. 2 *B*) is consistent with the recent

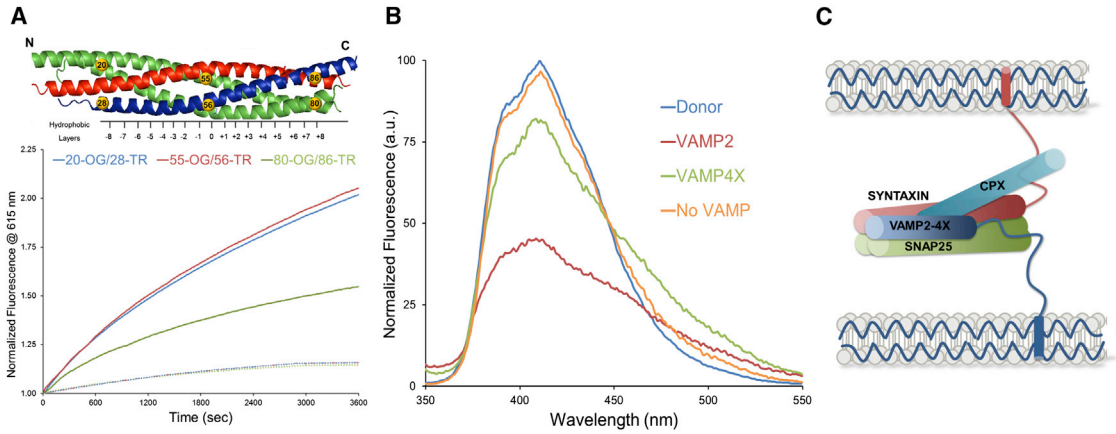

FIGURE 1 Prefusion CPX-SNARE complex assembled between Nanodiscs. (*A*) Assembly of SNAREs incorporated into Nanodiscs was followed by FRET between OG 488-labeled SNAP25 (t-SNARE) and TR-labeled VAMP2-4X. FRET (measured @ 615 nm, Ex 475 nm) for labels introduced at the N-terminus (20-OG/28-TR, *blue*), at the middle (55-OG/56-TR, *red*), and at the C-terminus (80-OG/86-TR, *green*) of the SNARE domain (*yellow circles*) are shown. The dashed lines (*same color coding*) represent the control experiment showing the effect of inclusion of the cytoplasmic domain of VAMP2 (CDV) to titrate out t-SNAREs and block assembly. (*B*) Stilbene-Bimane FRET experiments (12,36) probing the binding (and the conformational state) of CPX to SNAREpins assembled between Nanodiscs. Fluorescence emission spectra of CPX binding to the SNARE complexes assembled with v-discs containing VAMP2-4X (*green*), VAMP2 (*red*), or no VAMP2 (*orange*) are shown. Stilbene-Bimane FRET labels were introduced on SNAP25 (residue 193) and CPX (residue 38), respectively. A representative emission spectrum of a Stilbene (Donor)-only CPX-SNARE complex is shown in black. (*C*) Cartoon representation of the prefusion CPX-SNARE complex assembled between Nanodiscs (not drawn to scale), which mimics the clamped vesicle-bilayer junction, used in this study to follow the dynamics of the Ca^{2+}-activation of fusion by Synaptotagmin. Note: This is an idealized representation of the Nanodisc setup used merely to illustrate the experimental setup. The precise orientation of the Nanodiscs with respect to the SNAREs (and vice versa) is not known and other orientations are possible.

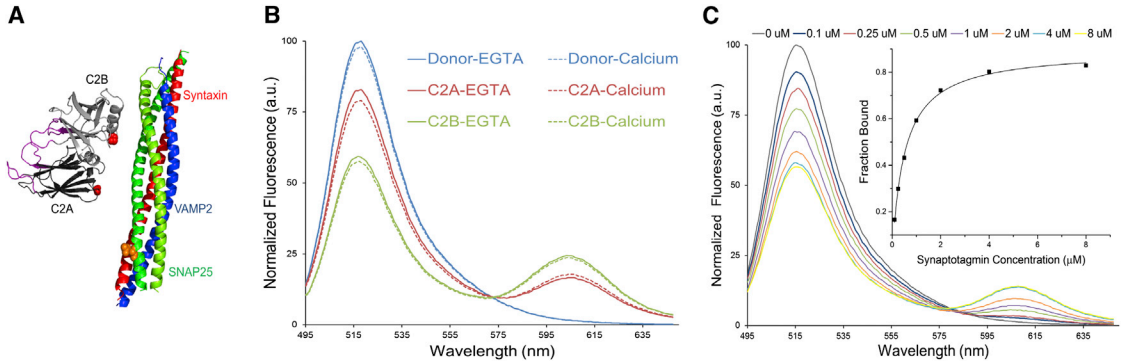

FIGURE 2 Synaptotagmin binds to the prefusion *trans* CPX-SNARE complex assembled between Nanodiscs (*A*) Model of SYT1-SNARE interaction (42,53) showing the FRET labeling sites. Donor, OG 488 was placed SNAP25 residue 76 (*orange spheres*) and acceptor, TR (*red spheres*) was attached to either the residue 154 (C2A) or residue 383 (C2B) of STY1. (*B*) Fluorescence emission curves for SYT1 binding to CPX-SNARE4X complex on Nanodiscs in the absence of Ca^{2+} (0.2 mM EGTA). Spectra for C2A label is shown in red, C2B label in green, and unlabeled (*donor-only*) in blue. Emission spectra of the same complexes following the addition of 1 mM free Ca^{2+} (*dashed lines*, *same color scheme*) are shown for comparison. (*C*) Titration of variable concentration of SYT1-383-TR into OG 488-labeled CPX-SNARE4X (SNAP25 76-OG) on Nanodiscs was used to measure the affinity of SYT1 to the prefusion CPX-SNARE complex in the absence of Ca^{2+} (0.2 mM EGTA). Inset: Quenching of donor fluorescence (as a function of the SYT1 concentration) was fitted to the standard single-site binding model to calculate the apparent affinity constants (Table 1). See Materials and Methods for fitting parameters.

smFRET demonstration (42) that the C2B domain of SYT1 interacts directly with the SNARE complex along its SNAP-25 surface, and that the C2A domain is more distant from the SNARE complex (42). To corroborate this, we studied and obtained similar results for SYT1 binding with other donor label positions (residue 54 on VAMP2-4X; Fig. S4).

Because we observed robust FRET with C2B domain labeling, we used the SNAP25-76/SYT1-383 label positions to further characterize the SYT1-SNARE interaction. Titration of variable SYT1 concentrations into CPX-SNARE4X complexes assembled between Nanodiscs reconstituted with 100% phosphatidylcholine (PC) bilayers yielded a saturable dose-response curve (Fig. 2 *C*), with an apparent affinity (K_d) ~0.7 μM (Table 1). Interestingly, we obtained identical binding curves, with K_d ~0.7 μM (Table 1) for SYT1 titrated into Nanodiscs containing either t-SNAREs alone (no v-discs included) or other SNARE complexes (SNARE4X, WT SNAREs—with or without CPX). This suggests that SYT1 primarily interacts with the t-SNARE portion of the SNARE complex and the positioning of SYT1 is unaffected by the zippering of the v-SNARE or the binding of CPX. Supporting this, we obtained comparable affinity constants (~0.6 μM) for the binding of SYT1 to isolated CPX-SNARE60 and CPX-SNARE complex (constructs used to obtain the prefusion (12) and postfusion (43) x-ray crystal structures, respectively) by SPR analysis under Ca^{2+} free conditions (Table 1; Fig. S5).

TABLE 1 Affinity constants (K_d) for Synaptotagmin binding to various CPX-SNARE complexes under Ca^{2+}-free conditions

SNARE complex	Binding affinity, K_d (μM)
Fluorescence measurement on Nanodiscs	
t-SNARE	0.73 ± 0.11
SNARE4X	0.71 ± 0.09
CPX-SNARE4X	0.68 ± 0.08
SNARE	0.72 ± 0.13
CPX-SNARE	0.65 ± 0.06
SPR (Biacore) measurement in solution	
CPX-SNARE60	0.65 ± 0.07
CPX-SNARE	0.64 ± 0.03

Quenching of the donor fluorescence ($SNAP25^{76}$-OG 488) as a function of the SYT1 (SYT^{383}-TR) concentration was used to calculate the apparent affinity (Fig. 2 *C*) of SYT1 to SNAREs on Nanodiscs. Biacore experiments were carried out with SYT1 binding to SNARE complexes captured on the sensor chips via biotin-streptavidin chemistry (Fig. S5). All binding studies were carried out in 25 mM HEPES, 50 mM KCl Buffer containing 0.2 mM EGTA.

Calcium activation: SYT1-membrane interaction

SYT1 binds Ca^{2+} at specific loops in its C2A and C2B domains so as to bridge these loops to acidic lipids such as PS and PIP_2 in the plasma membrane and/or synaptic vesicle (22,28,44–46). This strong interaction forces the loops into the adjacent lipid bilayer, a step which genetic evidence has shown to be essential for Ca^{2+}-triggered neurotransmitter release (13,31–33). Therefore, we tested if SYT1 bound to the half-zippered CPX-containing SNARE complex is still capable of inserting its loops into the membrane upon the binding Ca^{2+}? To do so, we introduced the environment-sensitive probe NBD in the Ca^{2+}-binding loops (47) of either the C2A (residue 234) or the C2B domain (residue 304) (Fig. 3 *A*). In steady-state fluorescence measurements with SYT1-CPX-SNARE4X complex preassembled between Nanodiscs (v- and t-discs each containing 15% PS), the NBD-probe on both C2 domains exhibited a Ca^{2+}-dependent increase in fluorescence intensity and blue shift in the emission spectrum (Fig. S6), consistent with Ca^{2+}-triggered penetration of Ca^{2+}-binding loops in to the lipid bilayer(s) (47).

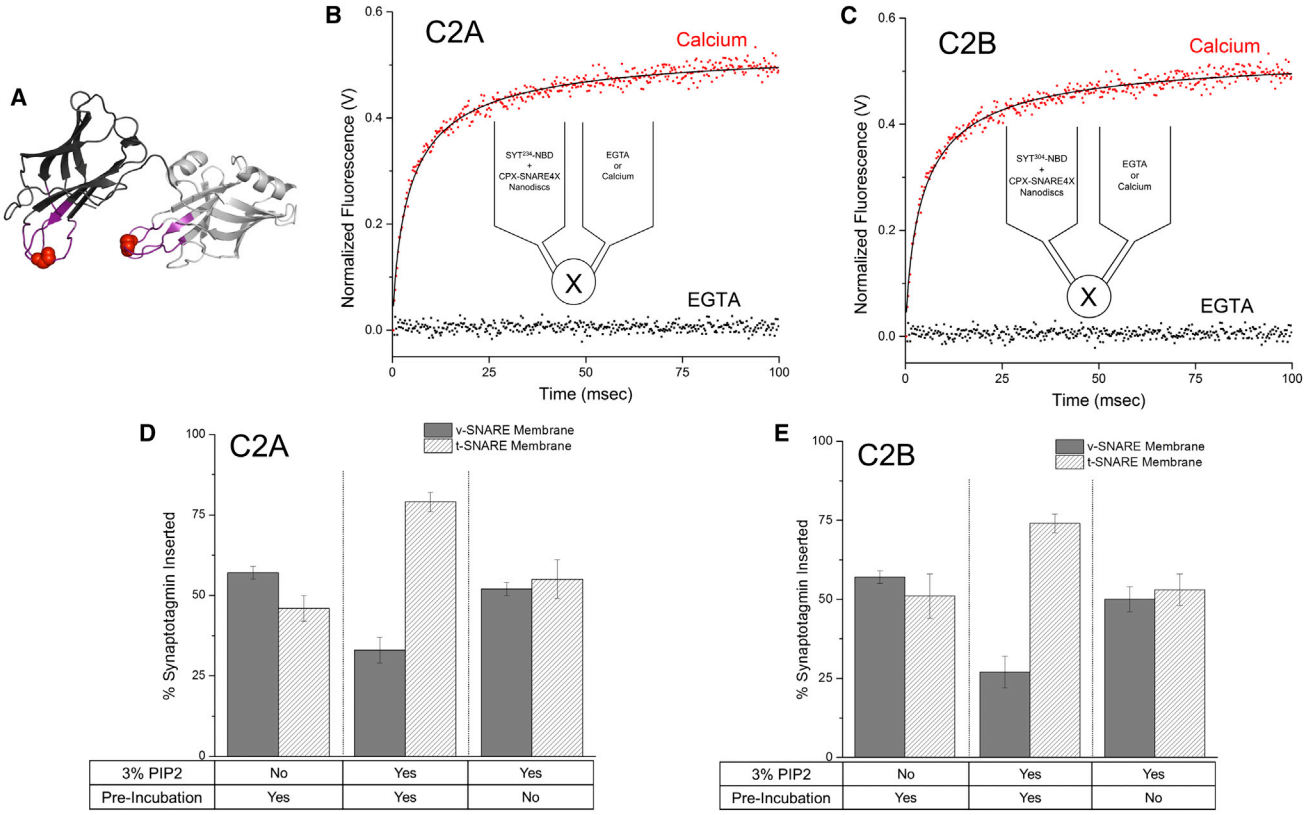

FIGURE 3 Ca^{2+}-triggered membrane interaction of Synaptotagmin. (*A*) Structural model of Synaptotagmin (adapted from (53)) depicting the NBD-labeling sites (*red spheres*) at the tip of the Ca^{2+}-binding loops (*purple*) used to monitor the membrane penetration activity of SYT1. Environment-sensitive probe NBD was attached to residue 234 on the C2A (*black*) or residue 304 on the C2B (*gray*) domain. (*B* and *C*) Dynamics of the membrane penetration of SYT1 bound to CPX-SNARE4X on Nanodisc upon Ca^{2+} addition measured using stopped-flow rapid mixing setup. The change in fluorescence signal of NBD (510 nm cutoff filter, Ex 460 nm) attached to the C2A (*B*) or C2B (*C*) domain was measured following rapid mixing (dead time = 1 msec) of samples yielding final concentrations of 0.2 mM EGTA (*black*) or 1 mM Ca^{2+} (*red*). The solid line represents the best fit of the corresponding data points using single exponential function. (*D* and *E*) Preferential insertion of the SYT1 Ca^{2+}-loops monitored by quenching of NBD fluorescence attached to the C2A (residue 234) or C2B (residue 304) domains by Rhodamine-PE (1.5%) introduced into either the v-disc (*solid*) or t-disc (*stripe*). Quenching of the NBD fluorescence was converted into the percentage of Synaptotagmin inserted into v-SNARE or t-SNARE membrane as described in the Materials and Methods section and Supporting Material (Fig. S7).

Stopped flow rapid-mixing analysis showed that the speed of this response satisfies the kinetic constraints of rapid neuronal exocytosis (Fig. 3, *B* and *C*). Ca^{2+} addition resulted in a very rapid change in the fluorescence signal for both the C2A and C2B labels (Fig. 3, *B* and *C*, respectively) with observed rate (K_{obs}) of 213 s^{-1} and 221 s^{-1}, respectively. The K_{obs} are very similar to that previously measured for interaction of soluble SYT1 with PC/PS liposomes (25). Thus, both C2 domains of SYT1 bound to the prefusion SNARE complex retain the unencumbered ability to insert very rapidly into the bilayer upon Ca^{2+} binding, the most critical element in the Ca^{2+}-activation process.

Quenching of the NBD signal by Rhodmaine-PE introduced specifically in the v-disc or the t-disc (assembled with lipid composition that accurately reflects the synaptic vesicle and the pre-synaptic plasma membrane respectively (20,48,49)), showed that the C2 domain has no inherent preference and insert into both v- and t-SNARE membrane equally (Fig. 3, *D* and *E*; Fig. S7) when the only anionic lipid present was PS (15% on both membranes). However, inclusion of PIP2 in the t-disc (because PIP2 is exclusively found on plasma membrane) resulted in a preferential insertion of the C2 domains into the t-disc (Fig. 3, *D* and *E*; Fig. S7) and this required the preincubation of SYT1 with CPX-SNARE4X Nanodiscs before the addition of Ca^{2+} (Fig. 3, *D* and *E*). This suggests that under physiological conditions (with 3–6% PIP2 in the plasma membrane (50)), the Ca^{2+}-independent mode of binding of SYT1 to PIP2 (22,28) might steer the membrane penetration of SYT1 toward the plasma membrane as opposed to the vesicle membrane.

Calcium activation: SYT1-SNARE interaction

Finally, we investigated the nature of the SYT1-SNARE interaction upon Ca^{2+} binding to understand how the rapid membrane insertion i.e., how the power stroke of SYT1 is coupled to the SNARE activation. To address this question,

we assembled the fluorescently labeled SYT1-CPX-SNARE4X complex between Nanodiscs in the presence of EGTA (0.2 mM). Steady-state FRET between OG 488-labeled SNAP25 (residue 76) in the SNARE complex and TR label on SYT1, in either its C2A (residue 154) or C2B (residue 383) domain (Fig. 2 *A*) was used to confirm the formation of this complex (Fig. 2 *B*). We then employed the stopped-flow rapid mixing technique to measure the positioning of SYT1 on the SNARE complex during the millisecond timescale process of SYT1 loops insertion into the Nanodisc bilayer(s) following the addition of Ca^{2+}. We observed no change in the donor fluorescence signal (OR) following the rapid mixing of Ca^{2+} (dead time ~1 ms) for either SYT1 C2A or C2B domain labels (Fig. 4, *A* and *B*), showing that both the C2A and the C2B domains remain bound in place on the SNARE complex relative to SNAP-25 during membrane insertion. Furthermore, FRET measurements using double fluorophore-labeled SYT1 C2 domain (Alexa 555-Alexa 647 labels on residue 254 on C2A and residue 396 on C2B) bound to the CPX-SNARE4X complex during Ca^{2+}-activation detected no internal rearrangements of the C2 domains even as it moves to insert rapidly into the bilayer (Fig. 4 *C*; Fig. S8). This suggests that SYT1 acts as a simple, rigid molecule that forcefully associates with the membranes while remaining in place on the assembling four-helix SNARE bundle, consistent with a mechanical forces model for Ca^{2+}-activation. Further supporting this, we observed no change in FRET signal following Ca^{2+} addition for both SYT1-SNAP25 (Fig. 2 *B*) and C2 dual labels under steady-state conditions (Fig. S8).

Previous studies have shown that Ca^{2+} enhances the binding of SYT1 to the SNAREs (37,46,51,52) and consistent with this finding, we observed increased affinity of SYT1 to different CPX-SNARE complex in the presence of 1 mM Ca^{2+} but only if Ca^{2+} was included during the binding of SYT1 to CPX-SNARE complex i.e., the incubation period (Fig. S9, Table S1). However, adding Ca^{2+} (1 mM) to SYT1-SNARE complex preassembled under Ca^{2+}-free conditions did not affect the SYT1-SNARE interactions (Fig. S9); particularly during the very rapid process of insertion of the SYT1 loops into the membrane bilayers.

DISCUSSION

Here, we show that in the absence of Ca^{2+}, SYT1 binds the partially assembled prefusion CPX-SNARE complex via its interactions with the t-SNAREs. Upon binding Ca^{2+}, SYT1 stays bound in place on the SNAREpins, but the Ca^{2+}-loops insert into the membrane bilayer with diffusion-limited kinetics. These findings place important and novel constraints on the activation mechanism, and combined with the previous structurally and biochemically established mechanism for clamping by CPX (11,12,36) suggest a simple physical process by which Synaptotagmin-Ca^{2+} could rapidly activate fusion from the clamped state. The CPX accessory helix clamps fusion by binding in *trans* to the C-terminal t-SNARE region on a neighboring SNAREpin, preventing its v-SNARE from completing its zippering (12). By virtue of this *trans*-clamping interaction, CPX organizes the SNAREpins into a zig-zag array at the vesicle-bilayer junction, which is topologically incompatible with opening of the fusion pore (12). The reversal of the CPX clamp requires an open to closed switch in the CPX's conformation that eliminates the *trans*- clamping interaction. However, this conformational switch requires three key Aspartate residues (residues 64, 65, and 68) found in the C-terminal portion of VAMP2 (between +2 and +4 hydrophobic layers) to be folded into the t-SNAREs (36). In the zig-zag array, each CPX is kept open by

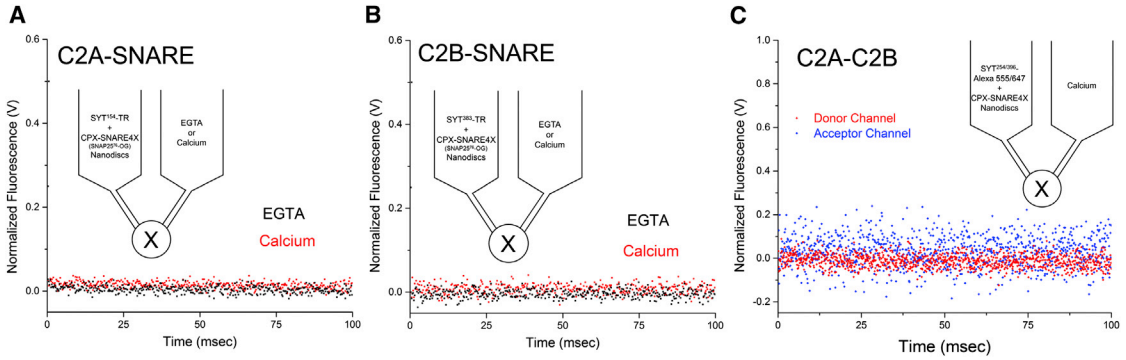

FIGURE 4 Synaptotagmin stays bound in place on the SNARE complex during the Ca^{2+}-activation process. (*A* and *B*) Positioning of the SYT1 on SNARE complex during the Ca^{2+} activation was monitored using a stopped-flow rapid mixing setup. SYT1 labeled with TR in the C2A domain (residue 154) or C2B domain (residue 383) was preincubated with OG 488-labeled CPX-SNARE4X (SNAP25 residue 76) on Nanodiscs and then the change in donor (OG 488) signal (515 nm cutoff filter, Ex 475 nm) was monitored following rapid mixing (dead time = 1 msec) of samples yielding final concentrations of 0.2 mM EGTA (*black*) or 1 mM Ca^{2+} (*red*). (*C*) Conformational dynamics of the C2 domain during Ca^{2+}-activation was monitored as outlined above but with unlabeled CPX-SNARE4X complex and SYT1 double-labeled with Alexa 555-Alex 647 donor-acceptor pair on C2A (residue 254) and C2B (residue 396). Fluorescence signal from both the donor (550 nm cutoff filter, *red*) and acceptor channel (620 nm cutoff filter, *blue*) excited at 530 nm following rapid mixing with 1 mM Ca^{2+} is shown.

trans-interaction of CPX_{acc} with the adjacent SNAREpin, which in turn prevents that SNAREpin's VAMP switch region from zippering. In essence, zippering of the VAMP switch region and the conformational switch in CPX are thermodynamically linked. Hence, the zig-zag array is only metastable and removal of even one SNAREpin from the array is expected to trigger its cooperative disassembly, releasing the SNAREpins to complete their zippering and trigger neurotransmitter release (36). Because, the zig-zag array is a nearly planar structure, pulling or twisting a SNAREpin is expected to dislodge it, requiring ~20 k_BT of free energy to break its two *trans*-accessory helix attachments (12,36).

We posit that SYT1 can bind the clamped zig-zag array without significantly perturbing it because SYT1 binds the SNARE complex along the SNAP25 helices, on the opposite side of the SNARE bundle from where CPX binds (42,53). Consistent with this, we could position SYT1 on the zig-zag array based on the recent Synaptotagmin crystal structure constrained with smFRET data (42,53) and the C2A and C2B domains fit on the zig-zag without any clashing between adjacent SYTs (Fig. 5 *A*). (Note: SYT1 can bind any (and all) of the SNAREpin in the zig-zag even though only two bound SYTs are shown in Fig. 5 *A*.) Significantly, with this arrangement, the polybasic motif (Lys-326, Lys-327, Lys-331) on C2B domain, which is critical for PIP2 binding (22,28) (Fig. 5 *A*, *orange*) and the Ca^{2+}-binding loops (Fig. 5 *A*, *red*) of both C2 domains are pointing away from the SNAREpins toward the membrane, free to interact with it. Specifically, our model is that when each (or any) SYT1 moves to rapidly insert its loops into the bilayer upon binding Ca^{2+}, that SNAREpin has an enhanced chance of being pulled away or out of planarity (or both) and is released from the zig-zag array, thereby triggering the concomitant cooperative disassembly of the entire clamped structure (Fig. 5 *B*). We hypothesize that this straightforward, one-step physical mechanism could explain how SYT1 rapidly activates neurotransmitter release—simply by removing its attached SNAREpin from clamped array by mechanical force. Each SNAREpin-attached SYT1 will provide at least 45 k_BT of free energy when it inserts its loops into PS/PIP2-containing bilayers at the intracellular concentration range of Ca^{2+} (36,54,55), sufficient to remove a SNAREpin out of the zig-zag array (~20 k_BT). Therefore, in our model, a single SYT1 binding to its complement of Ca^{2+} ions should be sufficient to trigger the release of the neurotransmitters.

In addition to removing the CPX clamp, SYT1 also acts on the membrane to accelerate the fusion event. Partial penetration of the Ca^{2+} loops into the bilayer causes local buckling of the membranes and this forced curvature is expected to facilitate bilayer merger, by lowering the activation energy for membrane fusion (29,30,34). It is noteworthy that, nonphysiologically—in the absence of CPX—SYT1 still triggers neurotransmitter release, although the release is less robust and asynchronous (20,56–59). It seems likely that this incomplete release process can employ the same mechanical principle we have elucidated here.

SUPPORTING MATERIAL

Nine figures and one table are available at http://www.biophysj.org/biophysj/supplemental/S0006-3495(13)01196-X.

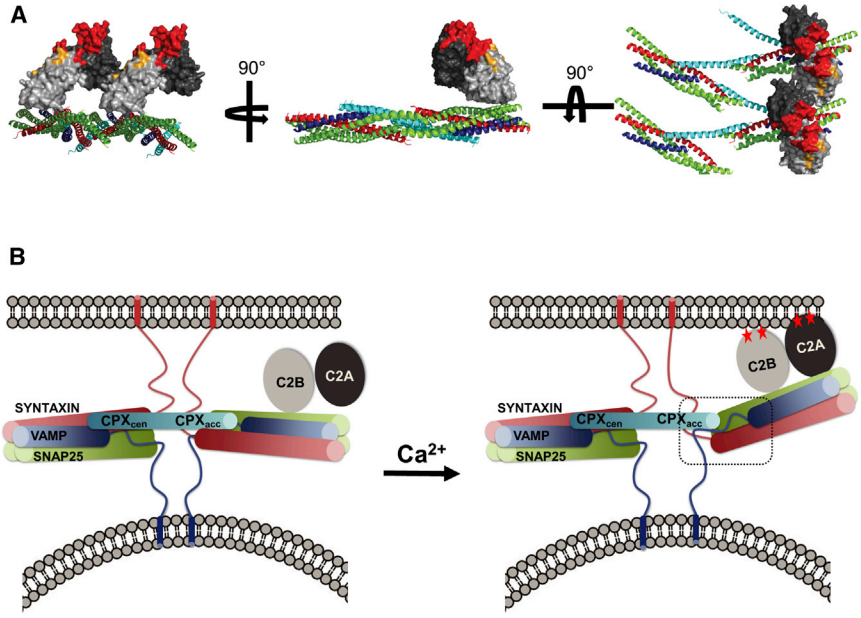

FIGURE 5 Model for the reversal of the CPX clamp by Synaptotagmin. (*A*) Representation of Synaptotagmin binding the clamped zig-zag array of prefusion CPX-SNARE complex at the vesicle-bilayer junction before the arrival of Ca^{2+} ions. SYT1 was modeled onto the zig-zag array using the x-ray structure and smFRET coordinates published recently (42,53). SYT1 binds to the SNAREs via its C2B domain (*gray*) and the polybasic motif, which interacts with PIP2 (*orange*) and the Ca^{2+}-binding loops on both C2 domains (*red*) are pointed away from the SNAREs ready to interact with the membranes. Note: We have modeled only two SYT1 binding to the zig-zag for illustrative purposes, but all the SNAREpins in the array are accessible. (*B*) In our model, when SYT1 binds Ca^{2+} (*red stars*), it moves rapidly to insert into the nearest bilayer along with the attached SNAREpin. This breaks the CPX_{acc}-SNARE clamping interaction (*dotted black box*) and removes the attached SNAREpin from the clamped zig-zag array. Removing a single CPX-SNARE complex would disrupt the interactions with both of its neighbors in the array, leading to cooperative disassembly of the entire zig-zag array, allowing the SNAREs to zipper fully and initiate fusion (36).

We thank J. Shen for providing the truncated t-SNARE expressing vector; F. Pincet, T. Melia, and E. Karatekin for helpful discussion and critical reading of the manuscript; and J. Rodriguez for providing some supporting data.

This work was supported by National Institutes of Health grant GM 071458 to J.E.R.

REFERENCES

1. Palade, G. E., and S. L. Palay. 1954. Electron microscope observations of interneuronal and neuromuscular synapses. *Anat. Rec.* 118:335–336.
2. Palay, S. L., and G. E. Palade. 1955. The fine structure of neurons. *J. Biophys. Biochem. Cytol.* 1:69–88.
3. DeRobertis, E. D. P., and H. S. Bennett. 1954. Submicroscopic vesicular component in the synapse. *Fed. Proc.* 13:35.
4. Fatt, P., and B. Katz. 1952. Spontaneous subthreshold activity at motor nerve endings. *J. Physiol.* 117:109–128.
5. Katz, B., and R. Miledi. 1965. The effect of calcium on acetylcholine release from motor nerve terminals. *Proc. R. Soc. Lond. B Biol. Sci.* 161:496–503.
6. Katz, B., and R. Miledi. 1967. The timing of calcium action during neuromuscular transmission. *J. Physiol.* 189:535–544.
7. Hu, C., M. Ahmed, …, J. E. Rothman. 2003. Fusion of cells by flipped SNAREs. *Science.* 300:1745–1749.
8. Söllner, T., S. W. Whiteheart, …, J. E. Rothman. 1993. SNAP receptors implicated in vesicle targeting and fusion. *Nature.* 362:318–324.
9. Weber, T., B. V. Zemelman, …, J. E. Rothman. 1998. SNAREpins: minimal machinery for membrane fusion. *Cell.* 92:759–772.
10. Giraudo, C. G., W. S. Eng, …, J. E. Rothman. 2006. A clamping mechanism involved in SNARE-dependent exocytosis. *Science.* 313: 676–680.
11. Li, F., F. Pincet, …, J. E. Rothman. 2011. Complexin activates and clamps SNAREpins by a common mechanism involving an intermediate energetic state. *Nat. Struct. Mol. Biol.* 18:941–946.
12. Kümmel, D., S. S. Krishnakumar, …, K. M. Reinisch. 2011. Complexin cross-links prefusion SNAREs into a zigzag array. *Nat. Struct. Mol. Biol.* 18:927–933.
13. Fernández-Chacón, R., A. Königstorfer, …, T. C. Südhof. 2001. Synaptotagmin I functions as a calcium regulator of release probability. *Nature.* 410:41–49.
14. Brose, N., A. G. Petrenko, …, R. Jahn. 1992. Synaptotagmin: a calcium sensor on the synaptic vesicle surface. *Science.* 256:1021–1025.
15. Geppert, M., Y. Goda, …, T. C. Südhof. 1994. Synaptotagmin I: a major Ca2+ sensor for transmitter release at a central synapse. *Cell.* 79:717–727.
16. Littleton, J. T., M. Stern, …, H. J. Bellen. 1994. Calcium dependence of neurotransmitter release and rate of spontaneous vesicle fusions are altered in *Drosophila* synaptotagmin mutants. *Proc. Natl. Acad. Sci. USA.* 91:10888–10892.
17. Pang, Z. P., O. H. Shin, …, T. C. Südhof. 2006. A gain-of-function mutation in synaptotagmin-1 reveals a critical role of Ca2+-dependent soluble *N*-ethylmaleimide-sensitive factor attachment protein receptor complex binding in synaptic exocytosis. *J. Neurosci.* 26:12556–12565.
18. Perin, M. S., V. A. Fried, …, T. C. Südhof. 1990. Phospholipid binding by a synaptic vesicle protein homologous to the regulatory region of protein kinase C. *Nature.* 345:260–263.
19. Giraudo, C. G., A. Garcia-Diaz, …, J. E. Rothman. 2009. Alternative zippering as an on-off switch for SNARE-mediated fusion. *Science.* 323:512–516.
20. Malsam, J., D. Parisotto, …, T. H. Söllner. 2012. Complexin arrests a pool of docked vesicles for fast Ca2+-dependent release. *EMBO J.* 31:3270–3281.
21. Südhof, T. C., and J. E. Rothman. 2009. Membrane fusion: grappling with SNARE and SM proteins. *Science.* 323:474–477.
22. Fukuda, M., T. Kojima, …, K. Mikoshiba. 1995. Functional diversity of C2 domains of synaptotagmin family. Mutational analysis of inositol high polyphosphate binding domain. *J. Biol. Chem.* 270:26523–26527.
23. Bai, J., C. A. Earles, …, E. R. Chapman. 2000. Membrane-embedded synaptotagmin penetrates *cis* or *trans* target membranes and clusters via a novel mechanism. *J. Biol. Chem.* 275:25427–25435.
24. Chapman, E. R., and A. F. Davis. 1998. Direct interaction of a Ca2+-binding loop of synaptotagmin with lipid bilayers. *J. Biol. Chem.* 273:13995–14001.
25. Davis, A. F., J. Bai, …, E. R. Chapman. 1999. Kinetics of synaptotagmin responses to Ca2+ and assembly with the core SNARE complex onto membranes. *Neuron.* 24:363–376.
26. Stein, A., A. Radhakrishnan, …, R. Jahn. 2007. Synaptotagmin activates membrane fusion through a Ca2+-dependent trans interaction with phospholipids. *Nat. Struct. Mol. Biol.* 14:904–911.
27. Hui, E., J. Bai, and E. R. Chapman. 2006. Ca2+-triggered simultaneous membrane penetration of the tandem C2-domains of synaptotagmin I. *Biophys. J.* 91:1767–1777.
28. Bai, J., W. C. Tucker, and E. R. Chapman. 2004. PIP2 increases the speed of response of synaptotagmin and steers its membrane-penetration activity toward the plasma membrane. *Nat. Struct. Mol. Biol.* 11:36–44.
29. Tucker, W. C., T. Weber, and E. R. Chapman. 2004. Reconstitution of Ca2+-regulated membrane fusion by synaptotagmin and SNAREs. *Science.* 304:435–438.
30. Martens, S., M. M. Kozlov, and H. T. McMahon. 2007. How synaptotagmin promotes membrane fusion. *Science.* 316:1205–1208.
31. Paddock, B. E., A. R. Striegel, …, N. E. Reist. 2008. Ca2+-dependent, phospholipid-binding residues of synaptotagmin are critical for excitation-secretion coupling in vivo. *J. Neurosci.* 28:7458–7466.
32. Paddock, B. E., Z. Wang, …, N. E. Reist. 2011. Membrane penetration by synaptotagmin is required for coupling calcium binding to vesicle fusion in vivo. *J. Neurosci.* 31:2248–2257.
33. Rhee, J. S., L. Y. Li, …, C. Rosenmund. 2005. Augmenting neurotransmitter release by enhancing the apparent Ca2+ affinity of synaptotagmin 1. *Proc. Natl. Acad. Sci. USA.* 102:18664–18669.
34. Chernomordik, L. V., and M. M. Kozlov. 2003. Protein-lipid interplay in fusion and fission of biological membranes. *Annu. Rev. Biochem.* 72:175–207.
35. Rathore, S. S., E. G. Bend, …, J. Shen. 2010. Syntaxin N-terminal peptide motif is an initiation factor for the assembly of the SNARE-Sec1/Munc18 membrane fusion complex. *Proc. Natl. Acad. Sci. USA.* 107:22399–22406.
36. Krishnakumar, S. S., D. T. Radoff, …, J. E. Rothman. 2011. A conformational switch in complexin is required for synaptotagmin to trigger synaptic fusion. *Nat. Struct. Mol. Biol.* 18:934–940.
37. Mahal, L. K., S. M. Sequeira, …, T. H. Söllner. 2002. Calcium-independent stimulation of membrane fusion and SNAREpin formation by synaptotagmin I. *J. Cell Biol.* 158:273–282.
38. Shi, L., Q. T. Shen, …, F. Pincet. 2012. SNARE proteins: one to fuse and three to keep the nascent fusion pore open. *Science.* 335:1355–1359.
39. Lakowicz, J. R. 2006. Principles of Fluorescence Spectroscopy. Springer, New York.
40. van de Weert, M., and L. Stella. 2011. Fluorescence quenching and ligand binding: A critical discussion of a popular methodology. *J. Mol. Struct.* 998:144–150.
41. Ritchie, T. K., Y. V. Grinkova, …, S. G. Sligar. 2009. Chapter 11 - Reconstitution of membrane proteins in phospholipid bilayer nanodiscs. *Methods Enzymol.* 464:211–231.
42. Choi, U. B., P. Strop, …, K. R. Weninger. 2010. Single-molecule FRET-derived model of the synaptotagmin 1-SNARE fusion complex. *Nat. Struct. Mol. Biol.* 17:318–324.
43. Chen, X., D. R. Tomchick, …, J. Rizo. 2002. Three-dimensional structure of the complexin/SNARE complex. *Neuron.* 33:397–409.

44. Damer, C. K., and C. E. Creutz. 1994. Synergistic membrane interactions of the two C2 domains of synaptotagmin. *J. Biol. Chem.* 269:31115–31123.

45. Araç, D., X. Chen, …, J. Rizo. 2006. Close membrane-membrane proximity induced by Ca(2+)-dependent multivalent binding of synaptotagmin-1 to phospholipids. *Nat. Struct. Mol. Biol.* 13:209–217.

46. Schiavo, G., Q. M. Gu, …, J. E. Rothman. 1996. Calcium-dependent switching of the specificity of phosphoinositide binding to synaptotagmin. *Proc. Natl. Acad. Sci. USA.* 93:13327–13332.

47. Hui, E., J. D. Gaffaney, …, E. R. Chapman. 2011. Mechanism and function of synaptotagmin-mediated membrane apposition. *Nat. Struct. Mol. Biol.* 18:813–821.

48. Takamori, S., M. Holt, …, R. Jahn. 2006. Molecular anatomy of a trafficking organelle. *Cell.* 127:831–846.

49. Cotman, C., M. L. Blank, …, F. Snyder. 1969. Lipid composition of synaptic plasma membranes isolated from rat brain by zonal centrifugation. *Biochemistry.* 8:4606–4612.

50. van den Bogaart, G., K. Meyenberg, …, R. Jahn. 2011. Membrane protein sequestering by ionic protein-lipid interactions. *Nature.* 479: 552–555.

51. Chapman, E. R., P. I. Hanson, …, R. Jahn. 1995. Ca2+ regulates the interaction between synaptotagmin and syntaxin 1. *J. Biol. Chem.* 270:23667–23671.

52. Bowen, M. E., K. Weninger, …, A. T. Brunger. 2005. Single-molecule studies of synaptotagmin and complexin binding to the SNARE complex. *Biophys. J.* 89:690–702.

53. Vrljic, M., P. Strop, …, A. T. Brunger. 2010. Molecular mechanism of the synaptotagmin-SNARE interaction in Ca2+-triggered vesicle fusion. *Nat. Struct. Mol. Biol.* 17:325–331.

54. Radhakrishnan, A., A. Stein, …, D. Fasshauer. 2009. The Ca2+ affinity of synaptotagmin 1 is markedly increased by a specific interaction of its C2B domain with phosphatidylinositol 4,5-bisphosphate. *J. Biol. Chem.* 284:25749–25760.

55. van den Bogaart, G., K. Meyenberg, …, R. Jahn. 2012. Phosphatidylinositol 4,5-bisphosphate increases Ca2+ affinity of synaptotagmin-1 by 40-fold. *J. Biol. Chem.* 287:16447–16453.

56. Jorquera, R. A., S. Huntwork-Rodriguez, …, J. T. Littleton. 2012. Complexin controls spontaneous and evoked neurotransmitter release by regulating the timing and properties of synaptotagmin activity. *J. Neurosci.* 32:18234–18245.

57. Lin, M. Y., J. G. Rohan, …, R. H. Chow. 2013. Complexin facilitates exocytosis and synchronizes vesicle release in two secretory model systems. *J. Physiol.* 591:2463–2473.

58. Diao, J., P. Grob, …, A. T. Brunger. 2012. Synaptic proteins promote calcium-triggered fast transition from point contact to full fusion. *Elife.* 1:e00109.

59. Xu, J., Z. P. Pang, …, T. C. Südhof. 2009. Synaptotagmin-1 functions as a Ca2+ sensor for spontaneous release. *Nat. Neurosci.* 12:759–766.